Global Change Biology

Global Change Biology (2013) **19**, 1470–1481, doi: 10.1111/gcb.12129

Local temperatures inferred from plant communities suggest strong spatial buffering of climate warming across Northern Europe

JONATHAN LENOIR*†, BENTE JESSEN GRAAE‡, PER ARILD AARRESTAD§, INGER GREVE ALSOS¶, W. SCOTT ARMBRUSTER‡‖**, GUNNAR AUSTRHEIM††, CLAES BERGENDORFF‡‡, H. JOHN B. BIRKS§§¶¶‖‖, KARI ANNE BRÅTHEN***, JÖRG BRUNET†††, HANS HENRIK BRUUN‡‡‡, CARL JOHAN DAHLBERG§§§, GUILLAUME DECOCQ†, MARTIN DIEKMANN¶¶¶, MATS DYNESIUS‖‖‖, RASMUS EJRNÆS****, JOHN-ARVID GRYTNES§§, KRISTOFFER HYLANDER§§§, KARI KLANDERUD§§†††††, MISKA LUOTO‡‡‡‡, ANN MILBAU§§§§, MARI MOORA¶¶¶¶, BETTINA NYGAARD****, ARVID ODLAND‖‖‖‖‖, VIRVE TUULIA RAVOLAINEN***, STEFANIE REINHARDT‖‖‖‖‖, SYLVI MARLEN SANDVIK*****, FRIDE HØISTAD SCHEI§§†††††, JAMES DAVID MERVYN SPEED††, LIV UNN TVERAABAK‡‡‡‡‡, VIGDIS VANDVIK§§, LIV GURI VELLE§§§§§, RISTO VIRTANEN¶¶¶¶¶, MARTIN ZOBEL¶¶¶¶ and JENS-CHRISTIAN SVENNING*

*Ecoinformatics & Biodiversity Group, Department of Bioscience, Aarhus University, Ny Munkegade 114, Aarhus C DK-8000, Denmark, †Ecologie et Dynamique des Systèmes Anthropisés (EA 4698), Plant Biodiversity Lab, Jules Verne University of Picardie, 1 rue des Louvels, Amiens Cedex 1 FR-80037, France, ‡Department of Biology, Norwegian University of Science and Technology NTNU, Trondheim NO-7491, Norway, §Norwegian Institute for Nature Research, PO Box 5685 Sluppen, Trondheim NO-7485, Norway, ¶Tromsø University Museum, Tromsø NO-9037, Norway, ‖School of Biological Sciences, University of Portsmouth, Portsmouth PO1 2DY, UK, **Institute of Arctic Biology, University of Alaska, Fairbanks AK 99775, USA, ††Museum of Natural History and Archaeology, Norwegian University of Science and Technology, Trondheim NO-7491, Norway, ‡‡Malmö Museer, Box 406, Malmö SE-201 24, Sweden, §§Ecological & Environmental Change Research Group, Department of Biology, University of Bergen, PO Box 7803, Bergen NO-5020, Norway, ¶¶Environmental Change Research Centre, University College London, Gower Street, London WC1E 6BT, UK, ‖‖School of Geography and the Environment, University of Oxford, South Parks Road, Oxford OX1 3QY, UK, ***Department of Arctic and Marine Biology, University of Tromsø, Tromsø NO-9037, Norway, †††Southern Swedish Forest Research Centre, Swedish University of Agricultural Sciences, Box 49, Alnarp SE-23053, Sweden, ‡‡‡Center for Macroecology, Evolution and Climate, Department of Biology, University of Copenhagen, Universitetsparken 15, Copenhagen Ø DK-2100, Denmark, §§§Department of Botany, Stockholm University, Stockholm SE-106 91, Sweden, ¶¶¶Institute of Ecology FB 2, University of Bremen, Leobener Str., Bremen DE-28359, Germany, ‖‖‖Department of Ecology and Environmental Science, Umeå University, Umeå SE-901 87, Sweden, ****Biodiversity & Conservation, Department of Bioscience, Aarhus University, Grenåvej 14, Rønde DK-8410, Denmark, ††††Department of Ecology and Natural Resource Management, Norwegian University of Life Sciences, PO Box 5003, Ås NO-1432, Norway, ‡‡‡‡Department of Geosciences and Geography, University of Helsinki, Helsinki FI-00014, Finland, §§§§Climate Impacts Research Centre, Department of Ecology and Environmental Science, Umeå University, Abisko SE-98107, Sweden, ¶¶¶¶Institute of Ecology and Earth Sciences, University of Tartu, Tartu EE-51005, Estonia, ‖‖‖‖Telemark University College, Bø NO-3800, Norway, *****Faculty of Engineering and Science, University of Agder, Service Box 422, Kristiansand NO-4604, Norway, †††††Norwegian Forest and Landscape Institute, Fanaflaten 4, Fana NO-5244, Norway, ‡‡‡‡‡Department of Education, University of Tromsø, Tromsø NO-9037, Norway, §§§§§Norwegian Institute for Agricultural and Environmental Research, Fureneset, Hellevik NO-6967, Norway, ¶¶¶¶¶Department of Biology, University of Oulu, Oulu FI-90014, Finland

Abstract

Recent studies from mountainous areas of small spatial extent (<2500 km^2) suggest that fine-grained thermal variability over tens or hundreds of metres exceeds much of the climate warming expected for the coming decades. Such variability in temperature provides buffering to mitigate climate-change impacts. Is this local spatial buffering restricted to topographically complex terrains? To answer this, we here study fine-grained thermal variability across a 2500-km wide latitudinal gradient in Northern Europe encompassing a large array of topographic complexities. We first combined plant community data, Ellenberg temperature indicator values, locally measured temperatures (LmT) and globally interpolated temperatures (GiT) in a modelling framework to infer biologically relevant temperature conditions from plant assemblages within <1000-m^2 units (community-inferred temperatures: CiT). We then assessed: (1) CiT range (thermal variability) within 1-km^2 units; (2) the relationship between CiT range and topographically

and geographically derived predictors at 1-km resolution; and (3) whether spatial turnover in CiT is greater than spatial turnover in GiT within 100-km^2 units. Ellenberg temperature indicator values in combination with plant assemblages explained 46–72% of variation in LmT and 92–96% of variation in GiT during the growing season (June, July, August). Growing-season CiT range within 1-km^2 units peaked at 60–65°N and increased with terrain roughness, averaging 1.97 °C (SD = 0.84 °C) and 2.68 °C (SD = 1.26 °C) within the flattest and roughest units respectively. Complex interactions between topography-related variables and latitude explained 35% of variation in growing-season CiT range when accounting for sampling effort and residual spatial autocorrelation. Spatial turnover in growing-season CiT within 100-km^2 units was, on average, 1.8 times greater (0.32 °C km^{-1}) than spatial turnover in growing-season GiT (0.18 °C km^{-1}). We conclude that thermal variability within 1-km^2 units strongly increases local spatial buffering of future climate warming across Northern Europe, even in the flattest terrains.

Keywords: climate change, climatic heterogeneity, community-inferred temperature, Ellenberg indicator value, plant community, spatial heterogeneity, spatial scale, temperature, topoclimate, topography

Received 27 November 2012; revised version received 27 November 2012 and accepted 14 December 2012

Introduction

Climate warming is a major threat to Earth's biodiversity (Fischlin *et al*., 2007; Rosenzweig *et al*., 2007). Several models using the IPCC climate-change scenarios to forecast impacts on biodiversity predict that many organisms risk extinction within the next century (Thomas *et al*., 2004; Thuiller *et al*., 2005). However, these models were computed at a coarse spatial resolution ($\gg$1 km^2) and fail to capture spatial variability in temperature over tens or hundreds of metres (Rae *et al*., 2006; Fridley, 2009; Randin *et al*., 2009; Ackerly *et al*., 2010; Fridley *et al*., 2011; Scherrer & Körner, 2011). Caution is therefore required in interpreting extinction predictions from these coarse-resolution models (Armbruster *et al*., 2007; Willis & Bhagwat, 2009; Hof *et al*., 2011; Schwartz, 2012).

Spatial variability in temperature at scales of as little as tens or hundreds of metres can potentially constitute an important buffer in ecosystem response to climate change (Ackerly *et al*., 2010). Such fine-grained thermal variability is usually attributed to physical processes such as air motion and solar radiation interacting with topographic complexities such as aspect, slope angle and roughness, i.e., topoclimate (Geiger & Aron, 2003). Topoclimatic variability may therefore provide microrefugia where species might persist locally amidst unfavourable regional climatic conditions (Dynesius *et al*., 2009; Ashcroft, 2010; Austin & Van Niel, 2011; Dobrowski, 2011) by shifting by as little as a few metres to neighbouring locations with cooler conditions (e.g., towards more polar-facing slopes with lower insolation or towards patches of wetter ground with higher heat-consuming evaporation) (Edwards & Armbruster, 1989; Wesser & Armbruster, 1991; Armbruster *et al*., 2007; Ackerly *et al*., 2010). Incorporating such topoclimatic processes into species distribution models predicts a greater local persistence of alpine and nival species in the Swiss Alps (Randin *et al*., 2009) where traditional species distribution models based on coarse climatic data predict extinction under the exact same future climate-change scenario (Ackerly *et al*., 2010). Focusing on a small mountainous landscape in California (250 km^2) (Van de Ven *et al*., 2007), Ackerly *et al*. (2010) assessed that thermal variability across this topographically complex area may increase from 3 to 8 °C if topoclimate variability is represented. Hitherto, the assessment of thermal buffering capacity over tens or hundreds of metres have been mostly limited to small spatial extents (<2500 km^2) and topographically complex terrains (Fridley, 2009; Ackerly *et al*., 2010; Scherrer & Körner, 2011). We are aware of only one study that provided fine-grained (625 m^2) topoclimatic grids of near-surface (5 cm) temperatures across a regional extent (60 000 km^2), while encompassing a wide range of topographic complexities from lowlands to highlands in Australia (Ashcroft & Gollan, 2012). Broad-scale assessments of fine-grained variability in temperatures and its variation across a large array of ecosystems are therefore lacking. Providing such assessments will help policy makers and landscape managers take critical decisions.

Miniature data-loggers and high-resolution thermal imagery are new tools that measure surface and soil temperatures with high precision allowing fine-scale spatial analysis of topoclimatic variability (Rae *et al*., 2006; Ashcroft *et al*., 2008; Fridley, 2009; Ackerly *et al*., 2010; Scherrer & Körner, 2011; Ashcroft & Gollan, 2012; Graae *et al*., 2012). However, the cost of using such tools across large geographic extents is still a limiting factor. In contrast, fine-grained (<1000 m^2) field surveys of plant community composition, which can be combined with species-indicator values for temperature (Ellenberg *et al*., 1992; Landolt *et al*., 2010) to infer thermal conditions (Scherrer & Körner,

Correspondence: Jonathan Lenoir, tel. 0033 7 62 82 94 40, fax 0033 3 22 82 54 21, E-mail: jonathan.lenoir@u-picardie.fr

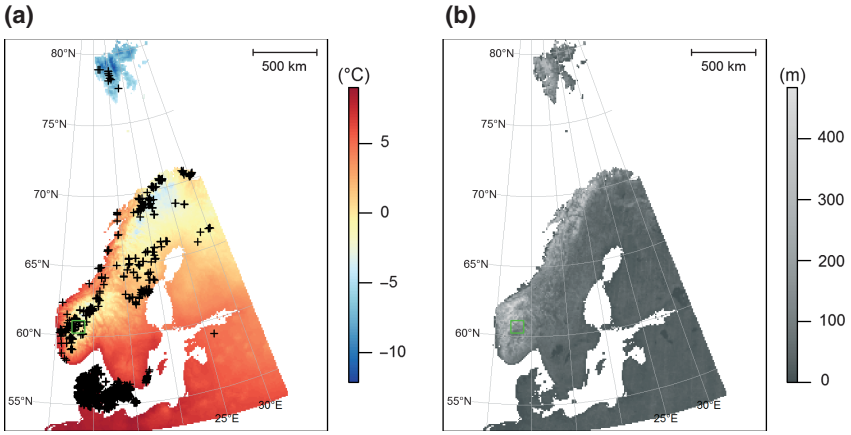

Fig. 1 Maps of (a) annual mean temperature conditions and (b) the range of elevation values within each 100-km^2 unit across the study area. Cross symbol gives the geographic location of all plant communities (n = 16 945). Green rectangles show the geographic location and spatial extent of the zooming windows used in Fig. 2.

2011), are available worldwide (Dengler *et al.*, 2011). Although this biotic approach does not directly estimate real temperature conditions as miniature data-loggers would, it estimates biologically relevant temperatures as mediated by the biological processes involved in plant community assembly. For these reasons, such community-based approaches have already been successfully implemented to map local bioclimatic heterogeneity within several small areas of 15 km^2 each in the Arctic (Karlsen *et al.*, 2005). Here, we first aim to infer temperature conditions from plant assemblages within <1000-m^2 units across a 2500-km wide latitudinal gradient in Northern Europe encompassing highly variable topographic complexity from flat to mountainous terrains. On the basis of these community-inferred temperatures (*CiT*), we then assess: (1) the spatial variability in *CiT* and thus buffering capacity within 1-km^2 units across this large region; (2) the relation between *CiT* variability and potential topographic and geographic drivers; and (3) whether spatial turnover in *CiT* within 100-km^2 units is greater than turnover computed from a 1-km temperature grid. If true, the latter would suggest that short-distance escapes for species facing climate change are likely underestimated by the 1-km gridded global climate surfaces.

Materials and methods

Study area

We focused on Northern Europe including Fennoscandia, Denmark and the Baltic countries (53–82°N, 3–32°E). This latitudinal gradient from the northern limit of the temperate biome (Denmark, Southern Sweden and the Baltic countries) to the northern limit of the Arctic biome (Svalbard) encompasses a large range of temperature conditions from 9.2 °C to −14.4 °C in annual mean temperatures and a large array of topographic variability from flat (e.g., Denmark and southern Finland) to mountainous (e.g., Norway and northern Finland) terrains (Fig. 1). Across our study area, we compiled data at three grain sizes: <1000 m^2; 1 km^2; and 100 km^2 (Fig. 2).

Vegetation, temperature and topographic data at the spatial grain of plant communities (<1000 m^2)

By updating an existing dataset in the Scandes (Lenoir *et al.*, 2010), we compiled a comprehensive database of 42 117 fine-grained (<1000 m^2) and geo-referenced plots of terrestrial vascular plant communities across Northern Europe encompassing a large array of vegetation types (forests, scrublands, grasslands, moorlands). All plots were imported to TURBOVEG (Hennekens & Schaminée, 2001). During the import procedure, all vascular taxa were linked to TURBOVEG's European species list, a list of valid names and synonyms based on Flora Europaea (Tutin *et al.*, 2001). We updated this list by adding taxa and synonyms not yet included. By relating all vegetation plots to this updated list, we ensured that the nomenclature was consistent. Then, we combined all vegetation plots with Ellenberg species-indicator values for temperature (Ellenberg *et al.*, 1992). Ellenberg *et al.* (1992) classified most of the plant taxa of Central Europe according to their optimal occurrence along key environmental gradients for plants. For temperature, they used an ordinal scale ranging from 1 (cold) to 9 (warm) in terrestrial environments. A total of 872 out of 1814 vascular plant taxa in our vegetation database had Ellenberg temperature indicator values. For each vegetation plot, we averaged the original Ellenberg temperature indicator values for the taxa present, excluding those lacking values. To estimate reliably Ellenberg averaged values (*EaV*) for temperature, we focused on vegetation plots with at least three taxa with Ellenberg values. In addition, we focused on vegetation plots with unique geographic coordinates and reliable information on location accuracy. A total of 16 945 (Fig. 1a) out of 42 117 vegetation plots met these criteria with location accuracy ranging from ±0.5 to ±500 m

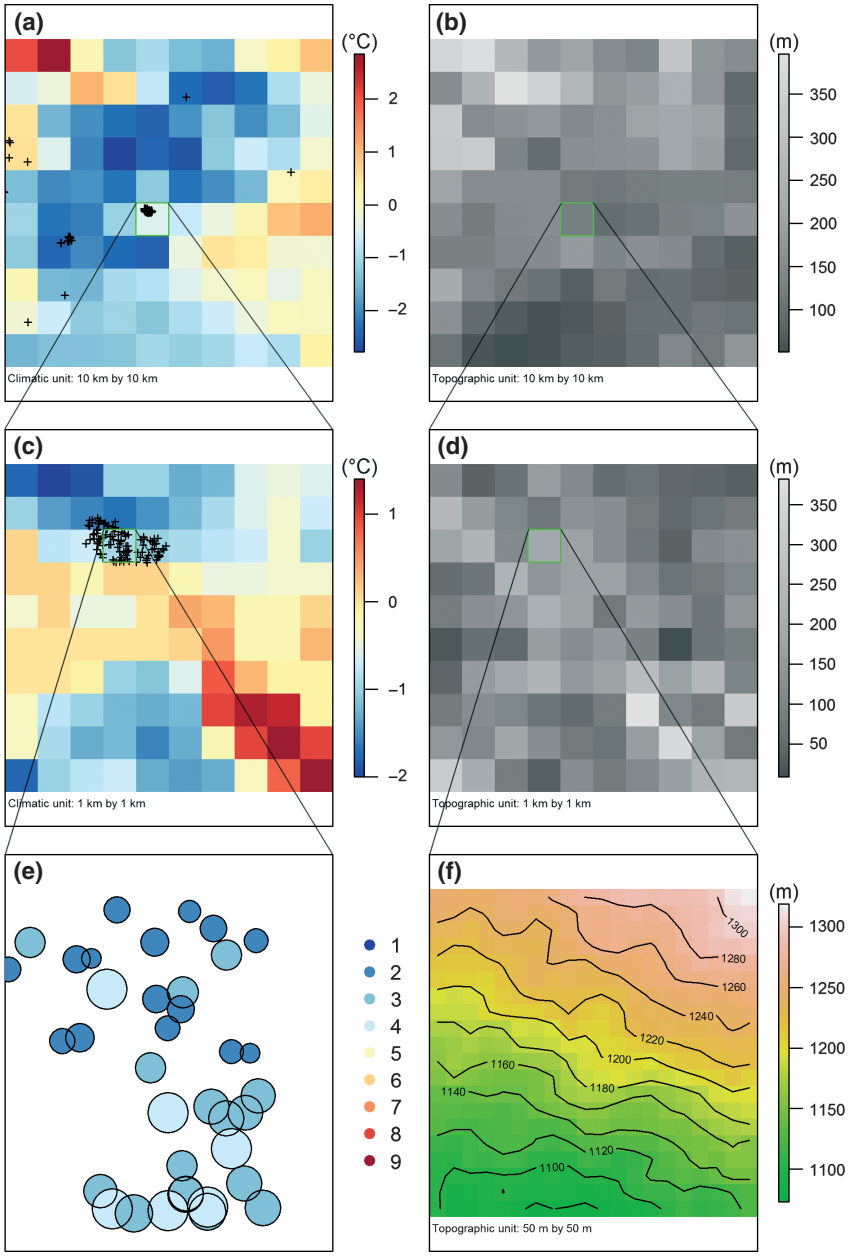

Fig. 2 Nested zooming windows illustrating the (a, b) 10-km, (c, d) 1-km and (e, f) 50-m resolution maps of (a, c, e) temperature and (b, d, f) elevation. Spatial distribution of (a, c) annual mean temperature conditions, (e) Ellenberg averaged values (EaV) for temperature, (b, d) the range of elevation values and (f) elevation across each zooming window are represented. Each pixel represents (a, b) a 100-km^2 unit, (c, d) a 1-km^2 unit or (f) a 2500-m^2 unit. Each circle represents a <1000-m^2 vegetation plot and its size is proportional to its EaV. Green rectangles show the location and spatial extent of the zooming windows used to depict scale nestedness.

(median = ±5 m, mean = ±15 m) and the number of taxa with Ellenberg values ranging from 3 to 50 (median = 7, mean = 9). The surface area (i.e., grain size) of these vegetation plots ranged from 0.1 to 900 m^2 (median = 79 m^2, mean = 79 m^2). Among the 16 945 selected plots, 138 had information on locally measured temperatures (*LmT*) from miniature soil data-loggers (Fig. S1). We focused on miniature soil data-loggers rather than miniature air data-loggers as soil temperature matters more than air temperature for most terrestrial vascular plants (Ashcroft *et al.*, 2008; Graae *et al.*, 2012). Monthly mean temperatures were extracted from each miniature soil data-loggers (Table S1).

To obtain topographic data, we used the fine-scale Advanced Spaceborne Thermal Emission and Reflection Radiometer (ASTER) Global Digital Elevation Model (GDEM) Version2 (Tachikawa *et al.*, 2011). We downloaded a total of 490 1° × 1° tiles to cover Northern Europe and processed each tile separately to control data quality and to compute four eleva-

tion-derivative indices at a 50-m resolution: slope, aspect, exposure to wind from the south-west and roughness (see Text S1 for data control and computational details). The exposure to wind is very different from aspect alone as it accounts for both slope and aspect to measure topographic sheltering from dominant winds (Ashcroft *et al*., 2008). For instance, within a region where south-west winds dominate, a site can have a south-west aspect directly facing dominant winds if one considers aspect solely, but be sheltered from these dominant winds if it is behind a mountain. High exposure values indicate high topographic sheltering effects and thus a more sheltered location (Ashcroft *et al*., 2008). Ashcroft *et al*. (2008) recommend using the exposure to wind to capture topographic complexities. We focused on exposure to the south-west solely because westerlies winds dominate across the study area.

Temperature and topographic data at the spatial grain of global climate surfaces (1 km^2 and 100 km^2)

We obtained temperature data from the WorldClim set of globally interpolated temperatures (*GiT*) (Hijmans *et al*., 2005). *GiT* are available as grid layers at a 30-arc-second resolution. These temperature grids are the basis for most species distribution modelling studies that predict the impact of future climate change on biodiversity (Thomas *et al*., 2004; Thuiller *et al*., 2005). Here, we used annual mean temperature and all 12 monthly mean temperature variables from historical baseline climatic conditions (1950–2000). Each of these 13 temperature grids was cropped to the study extent and resampled at an exact resolution of 1 km using the nearest neighbour resampling approach.

We also derived six grids reflecting topographic variability within each 1-km^2 unit. We first aggregated each of the 490 ASTER GDEM Version2 tiles at a 1-km resolution, computing the range of values (95th percentile − 5th percentile) for: elevation (*eleR*); slope (*slopR*); northness (*northR*); eastness (*eastR*); and exposure to the south-west (*expoR*) and computing the mean value for roughness (*roughM*). Because aspect values are circular, computing its range of values to reflect its variability within a 1-km^2 unit is not meaningful. Hence, we used cosine- and sine-transformed aspect values to reflect northness and eastness, respectively, before computing their ranges. We then created a composite grid, for each of the six topographically derived grids, by patching together the 490 tiles across Northern Europe. Finally, we resampled the composite grids at an exact resolution of 1 km using the nearest-neighbour resampling approach to match the resolution of the 13 temperature grids.

For the purpose of analysing spatial turnover in temperature conditions within 100-km^2 units, we aggregated each temperature and topographically derived grid at a 10-km resolution by computing the mean.

Data analysis

Inferring temperature conditions from plant assemblages. The first step of our analyses was to derive community-inferred temperatures (*CiT*) from the unitless *EaV* computed for each of the 16 945 vegetation plots. We obtained *CiT* by either: (1) fitting *LmT* from soil data-loggers against *EaV* in a 'bottom-up' approach or (2) fitting *GiT* from WorldClim temperature grids against *EaV* in a 'top-down' approach (see Text S2 for details on both the bottom-up and top-down modelling approaches).

Irrespective of modelling approach (bottom-up or top-down), *EaV* performed best to predict *CiT* during the growing season (June, July, August) (Figs. S2 and S3). For this reason and because growing-season mean temperatures are the most meaningful for plants, we decided to predict *CiT* from *EaV* by focusing on growing-season mean temperatures. Hence, we refitted *LmT* (bottom-up) and *GiT* (top-down) against *EaV*, but using this time the full set of data available for growing-season mean temperatures, i.e., 133 <1000-m^2 vegetation plots and 121 1-km^2 climatic units respectively. In addition, we tested for spatial autocorrelation in the residuals of these nonspatial models using Moran's *I* correlograms. Significance ($P < 0.05$) was evaluated by 1000 permutations for each distance class with correction of the resulting *P*-values for multiple comparisons using the Holm adjustment. In case of significant spatial autocorrelation in the first distance classes, we fitted spatial models to remove spatial autocorrelation from the residuals of the nonspatial models. We used the three nearest neighbours to build the spatial neighbourhood matrix and a row standardization (*W*) to generate the spatial weights matrix. On the basis of the spatial weights matrix, we used spatial eigenvector selection to reach a subset of significant ($P < 0.05$) spatial filters to be added in the formula of the nonspatial models (Bivand, 2009). We used the adjusted coefficients of either the nonspatial or spatial models to predict *CiT*. Finally, we averaged the bottom-up and top-down predicted values of *CiT* into a single *CiT* value of growing-season mean temperature for each of the 16 945 microclimatic units.

Assessing thermal variability. To evaluate thermal variability within 1-km^2 climatic units, we computed the range of values (maximum − minimum) for *CiT* within each 1-km^2 unit. To ensure a reliable estimate of thermal variability, we only used 1-km^2 units that included at least 10 vegetation plots. A total of 569 1-km^2 units met this criterion.

Relating thermal variability with topoclimate. We used generalized linear models to fit thermal variability within 1-km^2 climatic units (the response variable) against several variables reflecting topoclimate within the same spatial units. As a first set of topoclimatic variables, we conducted a Principal Component Analysis (*PCA*) on the six topographic grids (*eleR*, *slopR*, *roughM*, *northR*, *eastR*, *expoR*), covering a total of 1 905 865 1-km^2 climatic units, to reduce topographic complexity within each unit to a minimum set of composite and uncorrelated variables. The first two axes (PC_1 and PC_2) of the *PCA* were retained and accounted for 54% and 27% of the total variation respectively. PC_1 reflected the contributions of both elevation variability and slope variability (*eleR*, *slopR*, *roughM*) to topographic complexity within 1-km^2 climatic units, with the roughest units being located on the

positive end of PC_1 (Table S2). PC_2 reflected the contributions of variability in both exposure and aspect (*expoR*, *eastR*, *northR*) to topographic complexity within 1-km^2 climatic units, with units experiencing the largest heterogeneity in exposure being located on the positive end of PC_2 (Table S2). We also used the latitudinal position (*LP*) of each 1-km^2 climatic unit as an additional topoclimatically related variable reflecting a linear decrease in both: (1) solar angle from the equator to the poles and (2) daily-insolation contrasts between polar- and equator-facing slopes from 45°N to 90°N (Körner, 2003). As the probability of finding markedly different temperature conditions between two vegetation plots sampled within the same 1-km^2 climatic unit increases with sample size, we controlled for the effect of sampling effort (*SE*) on thermal variability within 1-km^2 units by using the number of vegetation plots sampled within each unit as a covariate in all our models. All four explanatory variables (PC_1, PC_2, *LP*, *SE*) were standardized to improve their interpretability (Schielzeth, 2010). As candidate models to explain thermal variability within 1-km^2 units, we tested all possible combinations (n = 18 models) of having 0, 1, 2 or 3 explanatory variables in addition to *SE*, including second- and third-order interaction terms between *LP*, PC_1 and PC_2. For model selection, we used Akaike's Information Criterion (*AIC*), with the Akaike weight (w) interpreted as the probability that a given model is the best among all candidate models (Burnham & Anderson, 2002). We tested for spatial autocorrelation in the residuals of the best candidate model and fitted a spatial model for the best candidate model only if there was significant spatial autocorrelation in the first distance classes (see above for a description on the implementation of spatial models).

Comparing spatial turnover in temperature with and without accounting for thermal variability within spatial units of global climate surfaces. For all pairwise comparisons of vegetation plots within a given 100-km^2 unit (Fig. S4), we computed: (1) the difference in growing-season *CiT*, which reflects the potential turnover in growing-season mean temperatures after accounting for thermal variability within 1-km^2 climatic units of WorldClim's global climate surfaces; (2) the difference in growing-season *GiT*, which reflects the actual turnover in growing-season mean temperatures across WorldClim's global climate surfaces at 1-km resolution; and (3) the geographical distance separating pairs of vegetation plots. We fitted an ordinary least-squares linear-regression model of the difference in *CiT* (resp. *GiT*) between pairs of vegetation plots (the response variables) against the geographical distance separating them (Fig. S4). Because of the nonindependence between paired differences, significance testing of the parameters of each model was obtained by running multiple linear regressions on distance matrices (Lichstein, 2007). We used 1000 permutations to estimate the statistical significance levels for each parameter. To fit a model of spatial turnover in temperature conditions within 100-km^2 units, we focused on 100-km^2 units that included at least 10 vegetation plots. A total of 349 units met this criterion. Finally, we compared estimates of the slope coefficients (°C m^{-1}) between both models of spatial turnover in growing-season *CiT* and *GiT*, but only for the subset of 100-km^2 units in which spatial turnover in growing-season *CiT* and *GiT* were significant ($P < 0.05$).

All WorldClim and ASTER GDEM Version2 raster layers were projected into the 'North Pole Lambert azimuthal equal-area Europe' projection in GRASS (Neteler & Mitasova, 2010) before being processed in R (R Development Core Team, 2011) for data handling and analyses using the 'ade4', 'ecodist', 'hexbin', 'ncf', 'raster', 'rgdal', 'sp' and 'spdep' packages.

Results

Focusing on the growing season (June, July, August) to predict community-inferred temperatures (*CiT*), we found positive relationships for both the bottom-up and top-down modelling approaches (Fig. 3). Ellenberg averaged values (*EaV*) explained 46% (adjusted $R^2 = 0.45$) of variation in locally measured temperatures (*LmT*) from miniature soil data-loggers and 92% (adjusted $R^2 = 0.92$) of variation in globally interpolated temperatures (*GiT*) from WorldClim respectively. Accounting for spatial autocorrelation by adding spatial filters as predictors in the nonspatial models improved the explanatory power, reaching 72% (adjusted $R^2 = 0.7$) and 96% (adjusted $R^2 = 0.96$) of variation in *LmT* and *GiT* respectively.

The span of values for growing-season *CiT* (thermal variability) within all 569 1-km^2 climatic units ranged from 0 to 6.57°C, averaging 2.1°C (SD = 0.97°C), across Northern Europe (Fig. 4).

Thermal variability increased linearly with sampling effort (*SE*) and roughness (PC_1), whereas its relationship with latitude (*LP*) was unimodal (Fig. 5). At intermediate latitudes (60–65°N), thermal variability averaged 2.72 °C (SD = 1.49 °C), reaching its maximum (6.57 °C) at 61°N (Fig. 5b). Thermal variability averaged 1.97 °C (SD = 0.84 °C) and 2.68 °C (SD = 1.26 °C) within the flattest ($PC1 < 0$) and roughest ($PC1 > 0$) 1-km^2 climatic units respectively (Fig. 5c). The second component of topographic complexity reflecting fine-grained (1 km^2) heterogeneity in exposure and aspect (PC_2) had no main effect on thermal variability (Fig. 5d). Using *SE* as a covariate, *LP* and PC_1 remained significant and models including both predictors had better support than others, among which the best candidate model showed a significant main effect for *LP* and significant multiplicative effects between PC_1 and PC_2 and between *LP*, PC_1 and PC_2 (Table 1). This complex model explained 23% (adjusted $R^2 = 0.22$) of the variation in thermal variability. Accounting for spatial autocorrelation by adding spatial filters as predictors in the best candidate model improved the explanatory power, reaching 35%

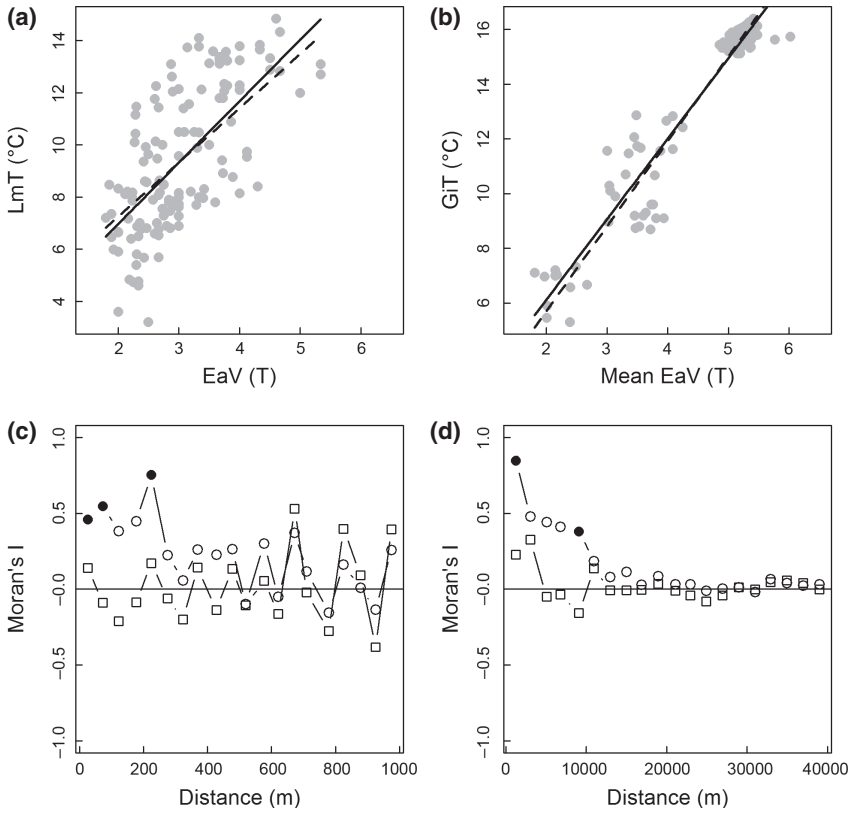

Fig. 3 Plots showing (a, b) fitted values and (c, d) correlograms of the residuals from the (a, c) bottom-up (n = 133 <1000-m^2 vegetation plots) and (b, d) top-down (n = 121 1-km^2 climatic units) models used to predict community-inferred temperatures during the growing season (June, July, August). EaV, LmT and GiT refer to Ellenberg averaged values, locally measured temperatures from miniature soil data-loggers, and globally interpolated temperatures from WorldClim respectively. Plain and dashed lines represent predictions from the nonspatial and spatial models respectively. Circles and squares represent Moran's I values from the nonspatial and spatial models respectively. Filled and open symbols represent significant ($P < 0.05$) and nonsignificant Moran's I values respectively.

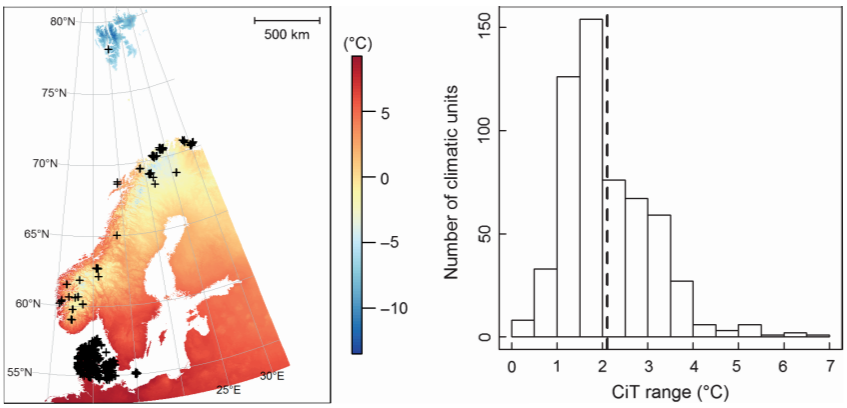

Fig. 4 Map and plot showing the (a) distribution of all 569 1-km^2 climatic units used to assess the range of values for community-inferred temperatures (CiT) and (b) a frequency histogram of the thermal variability (CiT range) within all these units. Background temperatures are 1-km^2 annual mean temperature from WorldClim. The dashed vertical line shows the mean.

(adjusted R^2 = 0.33) of the variation in thermal variability. Standardized partial regression coefficients were similar between the nonspatial and spatial models (Table 2).

Spatial turnover in growing-season mean temperatures was, on average, 1.8 times greater for *CiT* (0.32 °C km^{-1}) than for *GiT* (0.18 °C km^{-1}) (Wilcoxon signed-rank test: V = 1241, $P < 10^{-4}$).

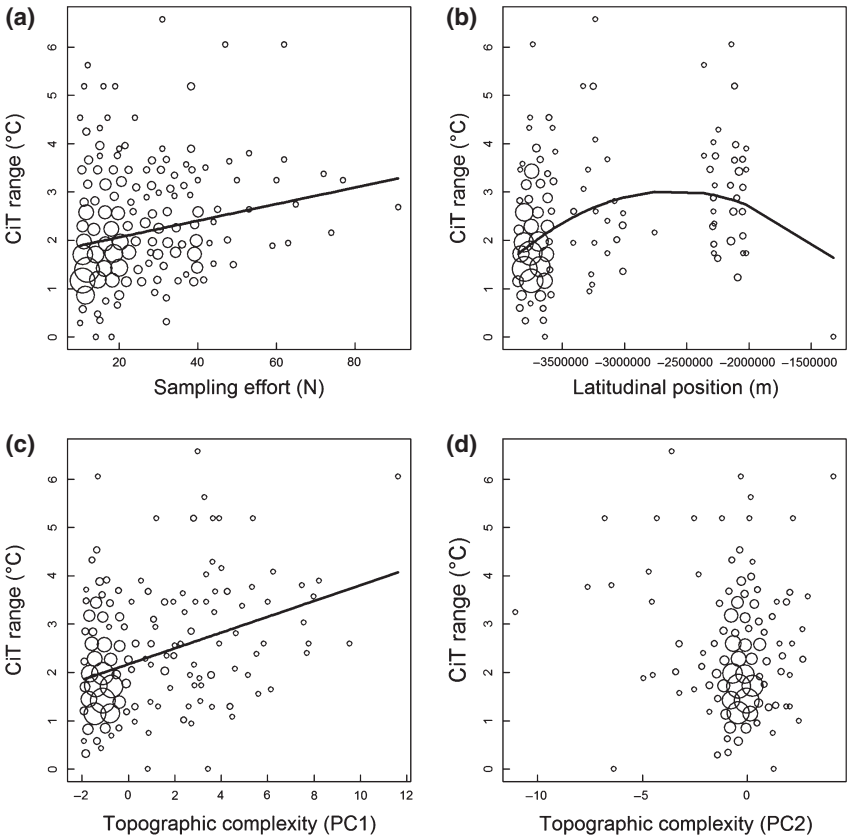

Fig. 5 Trends in the range of values for community-inferred temperatures (CiT) within each 1-km^2 climatic unit against various characteristics of these units: (a) sampling effort (SE); (b) latitudinal position (LP); (c) topographic heterogeneity due to elevation and slope (PC_1); and (d) topographic heterogeneity due to exposure and aspect (PC_2). Linear and quadratic trends were tested along each gradient and solid lines were added where significant ($P < 0.05$). Bubble size is proportional to the number of 1-km^2 climatic units falling within each bin of the *xy* plane tessellated by a regular grid of 26 by 21 hexagons [cf. 'hexbin' package in R (R Development Core Team, 2011)].

Discussion

The plant community-based approach

Our modelling results indicate that Ellenberg indicator values for temperature (Ellenberg *et al*., 1992) represent temperature conditions experienced by plants during the growing season (Fig. 3). Interestingly, the strength of the relationship between Ellenberg averaged values and locally measured growing-season mean temperatures from miniature soil data-loggers (R^2 ranging from 0.45 to 0.7) is similar to an earlier study relating Landolt indicator values for temperature (Landolt *et al*., 2010) with night-hours soil temperatures recorded between June and September ($R^2 = 0.51$) in the Swiss Alps (Scherrer & Körner, 2011). We furthermore found strong positive relationships (R^2 ranging 0.92–0.96) between Ellenberg averaged values and globally interpolated growing-season mean temperatures from WorldClim temperature grids in this study. Similarly, Karlsen & Elvebakk (2003) found strong positive relationships (R^2 ranging 0.82–0.92) between an empirical index of thermophily computed for 147 arctic plants and real temperature measurements from neighbouring meteorological stations in Greenland. Our study adds to a growing number of studies combining plant indicator values for temperature with independent data on field records of plant community composition (Karlsen & Elvebakk, 2003; Karlsen *et al*., 2005; Scherrer & Körner, 2011), an approach that is particularly well suited for predictive purposes.

We must emphasize that community-inferred temperatures tend to be conservative. Indeed, growing-season thermal variability within 1-km^2 climatic units assessed by means of community-inferred temperatures from a plant community-based approach was systematically lower than the one assessed by means of locally measured temperatures from miniature soil data-loggers (Fig. S5). This probably reflects that

Table 1 Model selection among 18 generalized linear models that explain thermal variability within 1-km^2 climatic units (n = 569) across Northern Europe. Rank of a given candidate model based on Akaike's Information Criterion (AIC), its difference to the best candidate model (ΔAIC) and its Akaike weight (w). Standardized partial regression coefficients are given for each explanatory variable. SE is the sampling effort (number of vegetation plots) within each 1-km^2 climatic unit. LP represents the latitudinal position of each 1-km^2 climatic unit. PC_1 and PC_2 are the first two axes of the Principal Component Analysis used to reduce topographic complexity within each 1-km^2 climatic unit to a minimum set of composite and uncorrelated variables. Second- and third-order interaction terms are tested between LP, PC_1 and PC_2. Grey partial regression coefficients are nonsignificant ($P \geq 0.05$)

SE	LP	PC_1	PC_2	LP : PC_1	LP : PC_2	PC_1 : PC_2	LP : PC_1 : PC_2	AIC	ΔAIC	w
0.19	0.30	0.09	−0.11	−0.04	−0.03	−0.25	0.14	1451	0.00	1
0.21	0.21	0.33	−0.25	−0.10	0.12			1474	23.21	0
0.20	0.16	0.21	−0.17		0.15	−0.06		1475	24.30	0
0.19	0.17	0.20	−0.22		0.11			1478	26.84	0
0.19	0.32		−0.20		0.10			1489	38.15	0
0.21	0.24	0.32	−0.15	−0.11		0.04		1489	38.26	0
0.21	0.22	0.27	−0.07	−0.07				1490	38.84	0
0.20	0.19	0.18	−0.06					1491	39.87	0
0.21	0.22	0.26		−0.07				1491	39.99	0
0.20	0.19	0.17						1491	40.46	0
0.19	0.19	0.18	−0.09			0.01		1493	41.53	0
0.19	0.32		−0.06					1499	47.89	0
0.20	0.32							1499	48.09	0
0.20		0.32	−0.06					1500	49.04	0
0.20		0.31						1501	49.55	0
0.20		0.32	−0.09			0.01		1502	50.72	0
0.20								1564	113.42	0
0.20			−0.04					1565	114.32	0

Table 2 Standardized partial regression coefficients, standard errors and associated P-values for each parameter of the spatial and nonspatial versions of the best candidate model. See Table 1 for a full description of each parameter

	Spatial			Nonspatial		
Parameter	Estimate	Standard error	P-value	Estimate	Standard error	P-value
Intercept	2.14	0.05	$< 10^{-4}$	2.15	0.05	$< 10^{-4}$
SE	0.18	0.03	$< 10^{-4}$	0.19	0.04	$< 10^{-4}$
LP	0.26	0.06	$< 10^{-4}$	0.30	0.06	$< 10^{-4}$
PC_1	0.14	0.09	0.15	0.09	0.09	0.32
PC_2	−0.09	0.06	0.18	−0.11	0.07	0.10
LP : PC_1	−0.03	0.05	0.46	−0.04	0.05	0.40
LP : PC_2	0.00	0.05	0.89	−0.03	0.05	0.51
PC_1 : PC_2	−0.23	0.05	$< 10^{-4}$	−0.25	0.05	$< 10^{-4}$
LP : PC_1 : PC_2	0.12	0.03	$< 10^{-4}$	0.14	0.03	$< 10^{-4}$

community-inferred temperatures from plant assemblages estimate thermal variability as filtered through biological community assembly processes. Indeed, abiotic variability will be smoothed out: (1) over space by metapopulation dynamics causing populations to average over fine-grained conditions and thus be dependent on the coarse-grain conditions (Eriksson, 1996; Freckleton & Watkinson, 2002) and (2) over time by species traits of perennial plants such as maturation time, dispersal ability and persistence capability causing plant assemblages to exhibit considerable lags in their response to climate variability (Bertrand *et al.*, 2011; Dullinger *et al.*, 2012). For these reasons, although the community-based approach underestimates real fine-grained (1 km^2) thermal variability, it may better reflects temperature conditions relevant to plant community dynamics than measurements from short-term, localized miniature soil data-loggers. Therefore, we propose that community-inferred temperatures provide a unique, highly valuable source of information to assess fine-grained (1 km^2) biologically relevant thermal variability.

Fine-grained (1 km^2) thermal variability in Northern Europe

Fine-grained variability in growing-season mean temperatures exceeds 2 °C in 44% of the 1-km^2 climatic units investigated (Fig. 4b). This suggests that many places across Northern Europe may provide substantial spatial buffering of the local impacts of climate change on species persistence. This result further argues for incorporating fine-grained thermal variability in predictive models of species distributions to provide more realistic projections of climate-change impacts (Van de Ven *et al*., 2007; Randin *et al*., 2009; Willis & Bhagwat, 2009; Ackerly *et al*., 2010). However, fine-grained thermal variability exceeding 4 °C is found in only 3% of the 1-km^2 climatic units investigated (Fig. 4b). This means that areas offering the high thermal variability necessary to cope with the range of warming projected by the IPCC scenarios of future climate change (IPCC, 2007) and avoid critical climate-change impacts (Schellnhuber *et al*., 2006) through local-scale relocation are scarce. Note, however, that our estimate of fine-grained thermal variability is conservative (Fig. S5). In addition, the probability that the most extreme sites with respect to temperature within each 1-km^2 climatic unit are included in the sample is low, although increasing with sampling effort (Fig. 5a).

Variation in fine-grained (1 km^2) thermal variability across Northern Europe and its potential determinants

As suggested by Scherrer & Körner (2011), our analyses of variation in thermal variability across Northern Europe show that as climate changes, rough terrains offer safer living conditions than flat terrains (Fig. 5c). Indeed a rough terrain provides a multitude of local temperature gradients over tens or hundreds of metres that are driven by topographic effects (Geiger & Aron, 2003; Ackerly *et al*., 2010) and may lower the regional risks of population decline under periods of extreme weather events, as well as under more gradual changes in climatic conditions, because climatically and ecologically different habitats are available for species within a close vicinity (Luoto & Heikkinen, 2008). Consistently, thermal variability peaks at 60–65°N (Fig. 5b), where rough terrains are predominant due to the gross topography from southern to mid-Norway. At about the same latitudes (66°N), Armbruster *et al.* (2007) found a maximum difference in direct-beam radiation budgets between polar- and equator-facing slopes thus suggesting high thermal variability. These radiation contrasts between polar- and equator-facing slopes coupled with the mountain-mass effect and strong North Atlantic climatic gradients from the ocean to the continent could underlie the high thermal variability we observed at these latitudes. Indeed, the confluence of these strong climatic gradients may contribute to the co-occurrence of both southern and northern plant species within a relatively small geographic area and thus locally inflate the size of the species pool (Zobel, 1997) and hence our plant community-based estimate of thermal variability at these latitudes. Overall, the availability of short-distance escapes for species facing climate change is likely to be higher at these latitudes.

Inconsistent with former studies that suggest that exposure and aspect represent different components of topoclimate that may increase fine-scale spatial heterogeneity in temperature (Ashcroft *et al*., 2008; Ashcroft & Gollan, 2012), our models do not suggest a positive main effect of spatial variability related to these topoclimatic components on thermal variability (Fig. 5d). Although exposure and aspect may influence temperature conditions, these factors may also influence water balance and soil conditions that interact with species distributions in ways that are not reflected by our community-inferred temperatures. However, our best model suggests that it is not via purely additive effects that the different drivers of topoclimate act, but rather *via* complex multiplicative effects among them (Table 1). On top of the positive main effect of latitude on thermal variability across Northern Europe, there is a positive three-way interaction between latitude, the elevation and slope components of topographic variability and the exposure and aspect components of topographic variability, even after accounting for other spatially structured effects (Table 2). In summer, the sun appears at a low angle above the horizon and at almost any aspect in high latitude areas. Topographic features being equal from 45 to 90°N, the linear decrease in solar angle is likely to intensify the positive effects of topographic complexity on thermal variability whereas the linear decrease in daily-insolation contrasts between polar- and equator-facing slopes is likely to mitigate the positive effects of topographic complexity on thermal variability. Given these compensating effects, our best model suggests that the intensifying effect of low solar angles on thermal variability overrides the mitigating effect of the sun appearing at almost any aspect towards the northern latitudes of the studied gradient.

By incorporating spatial filters in the nonspatial model to remove spatial autocorrelation in the residuals, we improved the explanatory power of our best model from 23% to 35%. This means that 12% of the variation is explained by one or several spatially autocorrelated explanatory variables missing in the nonspatial model and partly responsible for thermal variability within 1-km^2 climatic units. Among the potential

drivers that might be spatially autocorrelated, fine-scale spatial heterogeneity in canopy cover is likely to affect ground and air temperatures below the canopy (Geiger & Aron, 2003) and is often used as a predictor together with other topographic predictors to produce fine-resolution topoclimatic grids (Ashcroft & Gollan, 2012). For instance, trees and shrubs may strongly reduce the effect of topographically induced differences in insolation (Åström *et al.*, 2007). Therefore, not only topoclimate but also habitat heterogeneity may contribute to increase local spatial buffering of climate-change impacts on species, notably in the flattest terrains. Consistently, thermal variability reaches 1.97 °C, on average, within the flattest 1-km^2 climatic units investigated. This suggests that even the flattest terrains may still provide short-distance escapes for species facing climate change.

Fine-grained (1 km^2) thermal variability, global climate surfaces and spatial turnover in temperatures within 100-km^2 units

The spatial heterogeneity (turnover) in temperature conditions computed from community-inferred temperatures is almost twice the turnover computed from the WorldClim grid of globally interpolated temperatures. This suggests that species distribution models based on the WorldClim set of temperature grids tend to overestimate future species' range shifts in Northern Europe. Again, this argues for incorporating fine-grained thermal variability within models of species distribution (Randin *et al.*, 2009; Willis & Bhagwat, 2009; Ackerly *et al.*, 2010). In the context of contemporary climate change, fine-grained temperature turnover in space cannot be dissociated from temperature turnover in time at a given location. The ratio between temporal and spatial turnover in temperature determines the velocity of climate change and thereby how fast species will have to move to track suitable climate, determining the degree of threat (Loarie *et al.*, 2009). On the one hand, a higher level of threat is expected in flat terrains compared with rough ones which offer greater spatial turnover in temperature conditions for species facing climate change. On the other hand, a higher level of threat is expected for localities experiencing rapid climate change compared with localities experiencing a relatively stable climate. In short, flat terrains experiencing relative climate stability may be as safe places as rough terrains experiencing rapid climate change. Reflecting these two components of climate-change velocity, endemic species are globally concentrated in regions characterized by low Late Quaternary climate-change velocity (Sandel *et al.*, 2012). To improve predictions from future models of species distribution, both the fine-scale spatial and temporal components of the turnover in temperature conditions should therefore be incorporated.

Acknowledgements

The ideas for this manuscript were developed during meetings of the Stay or Go network funded by Nordforsk (Project Number 29662 to BJG). We thank the many people who collected data and those who in addition to the authors, managed and provided the databases that we used. Among them, we are particularly grateful to Marianne Iversen from the University of Tromsø, students from the University of Svalbard courses and the Norwegian Directorate for Nature Management (DN). We also thank David Ackerly and one anonymous referee for insightful comments and suggestions. We acknowledge a grant by the Danish Council for Independent Research – Natural Sciences (grant 272–07-0242 to JCS) and the European Regional Development Fund (Center of Excellence FIBIR).

References

Ackerly DD, Loarie SR, Cornwell WK, Weiss SB, Hamilton H, Branciforte R, Kraft NJB (2010) The geography of climate change: implications for conservation biogeography. *Diversity and Distributions*, **16**, 476–487.

Armbruster WS, Rae DA, Edwards ME (2007) Topographic complexity and biotic response to high-latitude climate change: variance is as important as the mean. In: *Arctic-Alpine Ecosystems and People in a Changing Environment* (eds Ørbæk JB, Kallenborn R, Tombre I, Hegseth EN, Falk-Petersen S, Hoel AH), pp. 105–122. Springer Verlag, Berlin Heidelberg, Germany.

Ashcroft MB (2010) Identifying refugia from climate change. *Journal of Biogeography*, **37**, 1407–1413.

Ashcroft MB, Gollan JR (2012) Fine-resolution (25 m) topoclimatic grids of near-surface (5 cm) extreme temperatures and humidities across various habitats in a large (200 × 300 km) and diverse region. *International Journal of Climatology*, **32**, 2134–2148. doi:10.1002/joc.2428

Ashcroft MB, Chisholm LA, French KO (2008) The effect of exposure on landscape scale soil surface temperatures and species distribution models. *Landscape Ecology*, **23**, 211–225.

Åström M, Dynesius M, Hylander K, Nilsson C (2007) Slope aspect modifies community responses to clear-cutting in boreal forests. *Ecology*, **88**, 749–758.

Austin MP, Van Niel KP (2011) Improving species distribution models for climate change studies: variable selection and scale. *Journal of Biogeography*, **38**, 1–8.

Bertrand R, Lenoir J, Piedallu C *et al.* (2011) Changes in plant community composition lag behind climate warming in lowland forests. *Nature*, **479**, 517–520.

Bivand R (2009) *Spdep: Spatial Dependence: Weighting Schemes, Statistics and Models. R Package Version 0.4-56*. The Comprehensive R Archive Network, Vienna, Austria.

Burnham KP, Anderson DR (2002) *Model Selection and Multimodel Inference: A Practical Information-Theoretic Approach*, 2nd edn. Springer-Verlag, NY.

Dengler J, Jansen F, Glöckler F *et al.* (2011) The Global Index of Vegetation-Plot Databases (GIVD): a new resource for vegetation science. *Journal of Vegetation Science*, **22**, 582–597.

Dobrowski SZ (2011) A climatic basis for microrefugia: the influence of terrain on climate. *Global Change Biology*, **17**, 1022–1035.

Dullinger S, Gattringer A, Thuiller W *et al.* (2012) Extinction debt of high-mountain plants under twenty-first-century climate change. *Nature Climate Change*, **2**, 619–622.

Dynesius M, Hylander K, Nilsson C (2009) High resilience of bryophyte assemblages in stream-side compared to upland forests. *Ecology*, **90**, 1042–1054.

Edwards ME, Armbruster WS (1989) A steppe-tundra transition on Kathul Mountain, Alaska. *Arctic and Alpine Research*, **21**, 296–304.

Ellenberg H, Weber HE, Düll R, Wirth V, Werner W, Paulißen D (1992) Zeigerwerte von Pflanzen in Mitteleuropa. *Scripta Geobotanica*, **18**, 1–248.

Eriksson O (1996) Regional dynamics of plants: a review of evidence for remnant, source-sink and metapopulations. *Oikos*, **77**, 248–258.

Fischlin A, Midgley GF, Price JT *et al.* (2007) Ecosystems, their properties, goods, and services. In: *Climate Change 2007: Impacts, Adaptation and Vulnerability. Contribution of Working Group II to the Fourth Assessment Report of the Intergovernmental Panel on*

Climate Change (eds Parry ML, Canziani OF, Palutikof JP, Van Der Linden PJ, Hanson CE), pp. 211–272. Cambridge University Press, Cambridge, UK.

Freckleton RP, Watkinson AR (2002) Large-scale spatial dynamics of plants: metapopulations, regional ensembles and patchy populations. *Journal of Ecology*, **90**, 419–434.

Fridley JD (2009) Downscaling climate over complex terrain: high finescale (<1000 m) spatial variation of near-ground temperatures in a montane forested landscape (Great Smoky Mountains). *Journal of Applied Meteorology and Climatology*, **48**, 1033–1049.

Fridley JD, Grime JP, Askew AP, Moser B, Stevens CJ (2011) Soil heterogeneity buffers community response to climate change in species-rich grassland. *Global Change Biology*, **17**, 2002–2011.

Geiger R, Aron RH (2003) *The climate near the ground*, 2nd edn. Harvard University Press, Cambridge, Massachusets.

Graae BJ, De Frenne P, Kolb A *et al.* (2012) On the use of weather data in ecological studies along altitudinal and latitudinal gradients. *Oikos*, **121**, 3–19.

Hennekens SM, Schaminée JHJ (2001) TURBOVEG, a comprehensive data base management system for vegetation data. *Journal of Vegetation Science*, **12**, 589–591.

Hijmans RJ, Cameron SE, Parra JL, Jones PG, Jarvis A (2005) Very high resolution interpolated climate surfaces for global land areas. *International Journal of Climatology*, **25**, 1965–1978.

Hof C, Levinsky I, Araújo MB, Rahbek C (2011) Rethinking species' ability to cope with rapid climate change. *Global Change Biology*, **17**, 2987–2990.

IPCC (2007) *Climate Change 2007: The Physical Science Basis*. Cambridge University Press, Cambridge, UK.

Karlsen SR, Elvebakk A (2003) A method using indicator plants to map local climatic variation in the Kangerlussuaq/Scoresby Sund area, east Greenland. *Journal of Biogeography*, **30**, 1469–1491.

Karlsen SR, Elvebakk A, Johansen B (2005) A vegetation-based method to map climatic variation in the arctic-boreal transition of Finnmark, north-easternmost Norway. *Journal of Biogeography*, **32**, 1161–1186.

Körner C (2003) *Alpine Plant Life*, 2nd edn. Springer-Verlag, Berlin, Heidelberg.

Landolt E, Bäumler B, Erhardt A *et al.* (2010) *Flora indicativa: Ecological indicator values and biological attributes of the flora of Switzerland and the Alps*. Haupt Verlag, Bern, Stuttgart, Wien.

Lenoir J, Gégout JC, Guisan A *et al.* (2010) Cross-scale analysis of the region effect on vascular plant species diversity in southern and northern European mountain ranges. *PLoS ONE*, **5**, e15734.

Lichstein JW (2007) Multiple regression on distance matrices: a multivariate spatial analysis tool. *Plant Ecology*, **188**, 117–131.

Loarie SR, Duffy PB, Hamilton H, Asner GP, Field CB, Ackerly DD (2009) The velocity of climate change. *Nature*, **462**, 1052–U111.

Luoto M, Heikkinen RK (2008) Disregarding topographical heterogeneity biases species turnover assessments based on bioclimatic models. *Global Change Biology*, **14**, 483–494.

Neteler M, Mitasova H (2010) *Open source GIS a GRASS GIS approach*, 3rd edn. Springer, New York.

R Development Core Team (2011) *R: A Language and Environment for Statistical Computing*. R Foundation for Statistical Computing. Vienna, Austria.

Rae DA, Armbruster WS, Edwards ME, Svengård-Barre M (2006) Influence of microclimate and species interactions on the composition of plant and invertebrate communities in alpine northern Norway. *Acta Oecologica*, **29**, 266–282.

Randin CF, Engler R, Normand S *et al.* (2009) Climate change and plant distribution: local models predict high-elevation persistence. *Global Change Biology*, **15**, 1557–1569.

Rosenzweig C, Casassa G, Karoly DJ *et al.* (2007) Assessment of observed changes and responses in natural and managed systems. In: *Climate Change 2007: Impacts, Adaptation and Vulnerability. Contribution of Working Group II to the Fourth Assessment Report of the Intergovernmental Panel on Climate Change* (eds Parry ML, Canziani OF, Palutikof JP, Van Der Linden PJ, Hansen CE), pp. 79–131. Cambridge University Press, Cambridge, UK.

Sandel B, Arge L, Dalsgaard B, Davies RG, Gaston KJ, Sutherland WJ, Svenning JC (2012) The influence of Late Quaternary climate-change velocity on endemism. *Science*, **334**, 660–664.

Schellnhuber HJ, Cramer W, Nakicenovic N, Wigley T, Yohe G (2006) *Avoiding Dangerous Climate Change*. Cambridge University Press, New York.

Scherrer D, Körner C (2011) Topographically controlled thermal-habitat differentiation buffers alpine plant diversity against climate warming. *Journal of Biogeography*, **38**, 406–416.

Schielzeth H (2010) Simple means to improve the interpretability of regression coefficients. *Methods in Ecology and Evolution*, **1**, 103–113.

Schwartz MW (2012) Using niche models with climate projections to inform conservation management decisions. *Biological Conservation*, **155**, 149–156.

Tachikawa T, Hato M, Kaku M, Iwasaki A (2011) *The Characteristics of ASTER GDEM Version 2*. IGARSS, Vancouver, Canada.

Thomas CD, Cameron A, Green RE *et al.* (2004) Extinction risk from climate change. *Nature*, **427**, 145–148.

Thuiller W, Lavorel S, Araújo MB, Sykes MT, Prentice IC (2005) Climate change threats to plant diversity in Europe. *Proceedings of the National Academy of Sciences of the United States of America*, **102**, 8245–8250.

Tutin TG, Heywood VH, Burges NA, Valentine DH, Walters SM, Webb DA (2001) *Flora Europaea 5 Volume Set and CD-ROM Pack*. Cambridge University Press, Mixed media, Cambridge, UK.

Van de Ven CM, Weiss SB, Ernst WG (2007) Plant species distributions under present conditions and forecasted for warmer climates in an arid mountain range. *Earth Interactions*, **11**, 1–33.

Wesser SD, Armbruster WS (1991) Controls over species distribution across a forest-steppe transition: a causal model and experimental test. *Ecological Monographs*, **61**, 323–342.

Willis KJ, Bhagwat SA (2009) Biodiversity and Climate Change. *Science*, **326**, 806–807.

Zobel M (1997) The relative role of species pools in determining plant species richness: an alternative explanation of species coexistence? *Trends in Ecology & Evolution*, **12**, 266–269.

Supporting Information

Additional Supporting Information may be found in the online version of this article:

Text S1. Data processing of each ASTER GDEM Version2 tile and computation of elevation-derivative variables.
Text S2. Bottom-up and top-down modelling approaches to predict community-inferred temperatures from Ellenberg averaged values.
Table S1. Characteristics of temperature data from miniature soil data-loggers.
Table S2. Correlation matrix of all the topographically related variables used to explain thermal variability.
Figure S1. Spatial distribution of the data used for calibration and validation of the bottom-up and top-down models.
Figure S2. Outputs from the calibration step of the bottom-up and top-down models.
Figure S3. Outputs from the validation step of the bottom-up and top-down models.
Figure S4. Spatial turnover in temperature conditions across 100-km^2 units.
Figure S5. Thermal variability within 1 km^2 climatic units: locally measured temperatures vs. community-inferred temperatures.